


## Article

# Simulation of Biocapacity and Spatial-Temporal Evolution Analysis of Loess Plateau in Northern Shaanxi Based on the CA–Markov Model

Hao Wang<sup>1,2,\*</sup>  and Yunfeng Hu<sup>1,2,\*</sup> 

<sup>1</sup> State Key Laboratory of Resources and Environmental Information System, Institute of Geographic Sciences and Natural Resources Research, Chinese Academy of Sciences, Beijing 100101, China

<sup>2</sup> College of Resources and Environment, University of Chinese Academy of Sciences, Beijing 100049, China

\* Correspondence: wanghao20@mails.ucas.ac.cn (H.W.); huyf@reis.ucas.ac.cn (Y.H.)

**Abstract:** Biocapacity evaluation is an important part of sustainable development research, but quantitative and spatial evaluation and future scenario analysis still have model and methodological difficulties. Based on the high-resolution Globeland30 dataset, the authors analyzed the characteristics of land use/cover changes of the Loess Plateau in Northern Shaanxi from 2000 to 2020. Then, comprehensively considering the driving factors of social development, topography, climatic conditions, and spatial distance, the logistic regression method and the CA–Markov model were used to simulate the land use scenario in 2030. Finally, the biocapacity model was used to describe the spatial distribution and spatial-temporal evolution of the regional biocapacity in detail. The results showed the following: (1) Biocapacity was jointly restricted by land use types, yield factors, and equivalence factors. The high values were mainly distributed in the riparian areas of the central and eastern regions, the ridges and valleys of the central and western regions, and the farmland patches of the southern valleys; the median values were mainly distributed in the forest of the southern mountains; the low values were mainly distributed in the grassland and unused land in the hilly and gully areas of the central and northern regions. (2) The biocapacity of Loess Plateau in Northern Shaanxi increased by 9.98% from 2000 to 2010, and decreased by 4.14% from 2010 to 2020, and the total amount remained stable. It is predicted that by 2030, the regional biocapacity will continue to increase by 0.03%, reaching  $16.52 \times 10^6$  gha.

**Keywords:** land use/cover; biocapacity; CA–Markov; Loess Plateau



**Citation:** Wang, H.; Hu, Y. Simulation of Biocapacity and Spatial-Temporal Evolution Analysis of Loess Plateau in Northern Shaanxi Based on the CA–Markov Model. *Sustainability* **2021**, *13*, 5901. <https://doi.org/10.3390/su13115901>

Academic Editors: Tomonobu Senjyu and Chunjiang An

Received: 1 April 2021

Accepted: 21 May 2021

Published: 24 May 2021

**Publisher's Note:** MDPI stays neutral with regard to jurisdictional claims in published maps and institutional affiliations.



**Copyright:** © 2021 by the authors. Licensee MDPI, Basel, Switzerland. This article is an open access article distributed under the terms and conditions of the Creative Commons Attribution (CC BY) license (<https://creativecommons.org/licenses/by/4.0/>).

## 1. Introduction

Since the 21st century, the contradiction between global economic and social development and resources and environment has become more prominent, and the international community has paid more and more attention to sustainable development. The United Nations has proposed global SDGs (sustainable development goals), and major countries in the world have also proposed national action plans. Sustainable development emphasizes the coordinated relationship between population, resources, environment, and development, and creates a healthy and sustainable resource and environmental foundation for future generations [1,2]. Biocapacity evaluation has become an important part of regional sustainable development research.

The theory of biocapacity and ecological footprint was first put forward by Rees et al. [3]. It emphasizes the material and energy basis of the operation of life systems, ecosystems, and human social systems [4]. In this theory, biocapacity quantifies the ability of ecology, environment, and resources to support the survival of humans and other organisms, and is a core indicator for evaluating the basis of regional sustainable development [5]. In recent years, scholars have studied biocapacity from different scales and perspectives, such as

regional biocapacity [6], national biocapacity [7], global biocapacity [8], spatial-temporal changes of biocapacity [9], and future simulation of biocapacity [10]. More importantly, scholars have conducted in-depth and extensive research on the effects of biocapacity stability and its changes, such as the restriction of biocapacity on economic growth and human capital [11,12], the impact of biocapacity changes on ecosystem services [13], the relationship between biocapacity and environmental management level [14], and the relationship between biocapacity and subjective well-being index [15]. These studies have enriched the theory and application of biocapacity, indicating that the stability of biocapacity plays an important role in the stability of ecological services, environmental improvement, and regional economic development. Their research results can provide a scientific basis for targeted governance by national and local governments, and are of great significance for the promotion of regional and global sustainable development.

In the calculation of biocapacity, the area and productivity of biologically productive land are basic elements [16]. Regional land use/cover change (LUCC) will directly cause changes in biocapacity and determine the spatial-temporal change pattern of biocapacity [17]. Therefore, historical land use data and future scenario data play an important role in the evaluation of biocapacity. Carrying out remote sensing interpretation of land use, or selecting land use data products with feasible accuracy and continuous time, to simulate future scenarios of LUCC, is the key to biocapacity prediction research.

In terms of land use simulation methods, the most widely used models include the CLUE-S (Conversion of Land Use and its Effects at Small Region Extent) model [18], Agent-CA (Agent-Cellular Automata) model [19], FLUS (Future Land Use Simulation) model [20], and CA-Markov (Cellular Automata-Markov) model [21]. The CLUE-S model integrates spatial analysis technology and the system theory method. It is a mature and widely used dynamic model, especially on a small area scale [22]. However, the CLUE-S model sets land use demand and elasticity coefficients based on personal experience, and its results are easily affected by subjective factors [23]. The Agent-CA model adds human and social factors to the natural and continuity simulation of the CA (Cellular Automata) model through the ABM (Agent-Based Model), which can easily explore urban land development scenarios under different policies [24]. However, the ABM relies on survey data to define the agent's behavioral rules, and the simulation results are highly subjective [23]. The FLUS model uses an ANN (Artificial Neural Network) to calculate land suitability, and then uses a CA model with an adaptive inertial mechanism to simulate land use changes [25,26]. The ANN brings the land suitability assessment closer to human thinking, but there is also a "black box" problem, which is that researchers cannot know the mechanism of land use change. The CA-Markov model organically combines the long-term prediction advantage of the Markov model with the complex system simulation capability of the CA model [27,28]. It uses the Markov area transfer matrix as the area evolution target of the CA model [29], which solves the key problem that LUCC simulation has difficulty achieving spatial-temporal synchronization, and the simulation effect is excellent [30].

The Loess Plateau in Northern Shaanxi is the core area of China's Loess Plateau. The Cenozoic red soil layer and the loose loess layer, with a thickness of dozens to more than 100 m, cover the Mesozoic bedrock foundation. After a long period of water cutting, soil erosion, and human activities, the unique landform of "hundreds and thousands of hills and valleys" is finally formed. On the whole, the vegetation in this area has been widely destroyed, the soil erosion is serious, and the ecological environment is fragile. In 1999, the Chinese government launched the GGP (the Grain to Green Program), trying to restore part of the farmland to forest and grassland to improve the regional ecological environment [31]. In recent years, scholars have studied the effects of the GGP implementation and changes in the regional ecological environment from multiple aspects such as vegetation coverage [32], soil and water conservation [33], and ecological services [34]. Relevant results show that, since 2000, the soil and water conservation capacity of the Loess Plateau has been significantly enhanced, vegetation restoration and soil erosion control have achieved good results [33], regional hydrological regulation capacity has

been significantly improved, carbon storage has increased [34], and vegetation coverage and vegetation quality has improved [32]. These in-depth and detailed studies provide a scientific basis for the government to formulate policies for ecological construction, regional planning, and sustainable development. However, the existing research also has some shortcomings, such as focusing more on historical processes rather than future trends, single ecosystem types and processes rather than complex changes in multiple ecosystem types, and environmental protection policy and environmental performance evaluation rather than quantitative study of biocapacity.

Given the insufficient quantitative analysis of biocapacity, insufficient understanding of spatial distribution laws, and insufficient clarity of future development trends in the study of sustainable development of the Loess Plateau, this article applies the logistic regression method to grasp the laws of LUCC based on authoritative land use data. Furthermore, we apply the CA–Markov model and biocapacity model to carry out a quantitative and spatial analysis of the future land use and biocapacity of the Loess Plateau in Northern Shaanxi. The research aims to answer the following three key questions:

- (1) How to construct a set of biocapacity evaluation models suitable for the Loess Plateau in Northern Shaanxi?
- (2) What will be the spatial distribution pattern of the biocapacity of the Loess Plateau in Northern Shaanxi in the future?
- (3) In response to future changes in the biocapacity, what strategies should the government take?

## 2. Study Area, Data, and Methods

### 2.1. Study Area

The Loess Plateau in Northern Shaanxi (Figure 1) includes 25 counties (districts) in Shaanxi Province in administrative divisions, with a total area of about 80,000 km<sup>2</sup>, accounting for about 39% of the total area of Shaanxi Province. It is located in the core area of China's Loess Plateau and is on the edge of the temperate monsoon climate zone. Its latitude and longitude range are roughly 107°15' E–111°15' E and 35°21' N–39°35' N. The annual average temperature is 7–11 °C, the annual precipitation is 300–600 mm, the climate is dry, the evaporation rate is high, and the frost-free period is short. It is a typical arid and semi-arid area in Northwest China. The terrain of the region is higher in the northwest and lower in the southeast, and the altitude is mostly between 1000 and 2000 m. The basic landform types include loess tableland, loess ridge, loess hill, and loess gully, which form the plateau surface of the Loess Plateau after modern gully segmentation.

The Loess Plateau in Northern Shaanxi has many rivers and fertile soil. It is called “the granary in the Loess Plateau”. In 2018, the Loess Plateau in Northern Shaanxi had a total population of 6.18 million, accounting for 16% of Shaanxi Province, the GDP was RMB 540.8 billion, accounting for 22% of Shaanxi Province; the per capita GDP was RMB 96,212—1.52 times the per capita GDP of Shaanxi Province; and the grain output was 3.36 million tons, accounting for 27% of Shaanxi Province.

### 2.2. Basic Data and Pre-Processing

The land use/cover data used in this study are from the Globeland30 data set provided by the China State Geospatial Information Center (<http://www.globallandcover.com/>, accessed on 28 September 2020) [35]. The resolution is 30 m. The Globeland30 data set has been sent to the United Nations by the Chinese government for free use by all countries [36–39]. In this study, 10 land types in the original Globeland30 data were reclassified into six categories (farmland, forest, grassland, water area, built-up land, and unused land), and binary images of these six types of land were made.

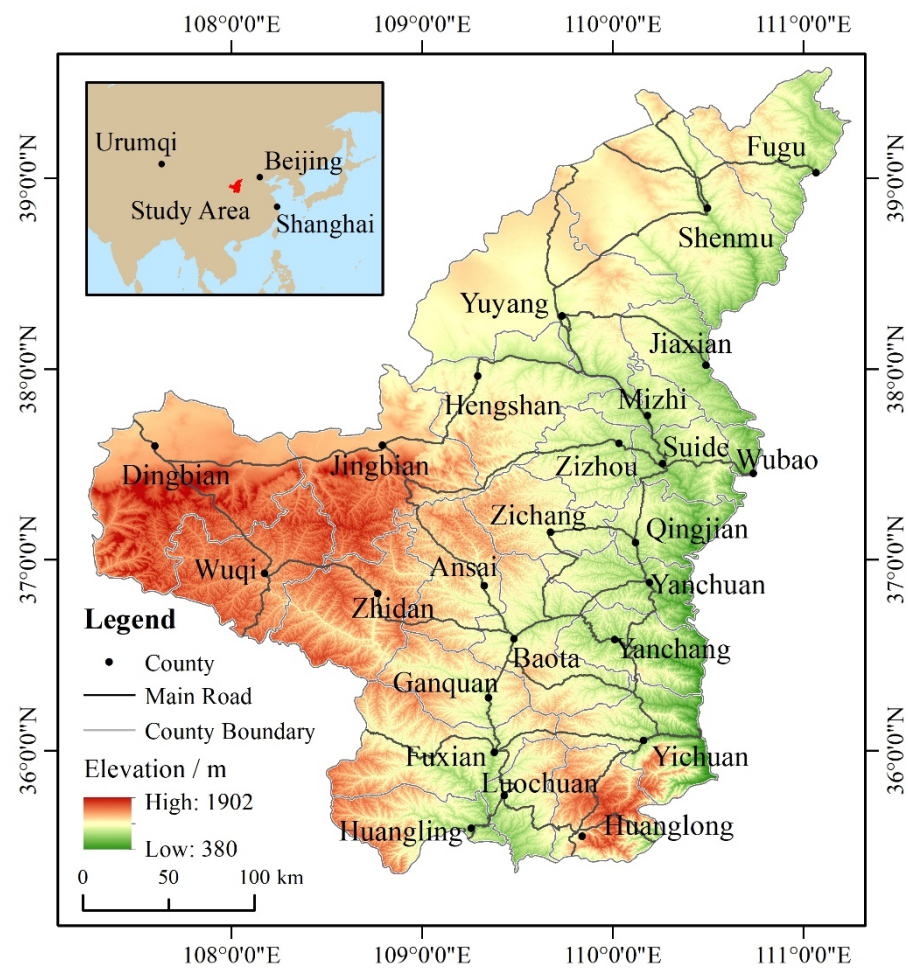


**Figure 1.** The location and topography of the Loess Plateau in Northern Shaanxi.

Selecting and determining the driving factors of LUCC is the key to accurately simulating future scenarios. This study referred to the experience of scholars in similar areas [40–42], and comprehensively considered the characteristics of economic and social development in Northern Shaanxi. A total of 10 factors in four categories were selected as the key driving factors for LUCC. The detailed information and processing methods of the driving factors are shown in Table 1.

**Table 1.** Driving factors of LUCC of the Loess Plateau in Northern Shaanxi.

Categories	Factors	Data Sources	Processing Methods	Final Results
Economic and social development	Per capita GDP	Resource and Environment Science and Data Center ( <a href="http://www.resdc.cn/">http://www.resdc.cn/</a> , accessed on 5 October 2020), National Per capita GDP data with 1 km resolution in 2010 and 2015	Linear interpolation, resample	Per capita GDP data in 2010 and 2020
	Population density	Resource and Environment Science and Data Center, National population density data with 1 km resolution in 2010 and 2015	Linear interpolation, resample	Population density data in 2010 and 2020
Topography	Elevation	Geospatial Data Cloud ( <a href="http://www.gscloud.cn/">http://www.gscloud.cn/</a> , accessed on 8 October 2020), DEM data	Mosaic, clip, projection	Elevation data
	Slope	Calculated by DEM data		Slope data
	Aspect	Calculated by DEM data		Aspect data

Table 1. Cont.

Categories	Factors	Data Sources	Processing Methods	Final Results
Climatic condition	Annual precipitation	Greenhouse Data Sharing Platform ( <a href="http://data.sheshiyuanyi.com/">http://data.sheshiyuanyi.com/</a> , accessed on 16 October 2020), annual precipitation observation data of 16 meteorological stations in the study area and surrounding area from 2010 to 2019	Linear interpolation, IDW interpolation	Annual precipitation data from 2010 to 2020
	Annual accumulated temperature (>10 °C)	Greenhouse Data Sharing Platform, annual accumulated temperature observation data of 16 meteorological stations from 2010 to 2019	Linear interpolation, IDW interpolation	Annual accumulated temperature data from 2010 to 2020
Spatial distance relationship	Distance to main roads	National Basic Geographic Information Database	Euclidean distance	Distance to main roads data
	Distance to rivers	National Basic Geographic Information Database	Euclidean distance	Distance to rivers data
	Distance to built-up land	GlobeLand30 dataset	Resample and Euclidean distance	Distance to built-up land data in 2010 and 2020

The general statistical work of the basic data was completed in MS Excel; spatial statistics and interpolation analysis were completed in ArcGIS 10.8; the final results were all raster data with a resolution of 30 m.

We standardized the driving factor data, and then used IDRISI32 software and logistic regression to make suitability maps for various types of land.

### 2.3. Research Methods

#### 2.3.1. Analytical Framework and Methods

The main analytical framework and methods of this study is shown in Figure 2.

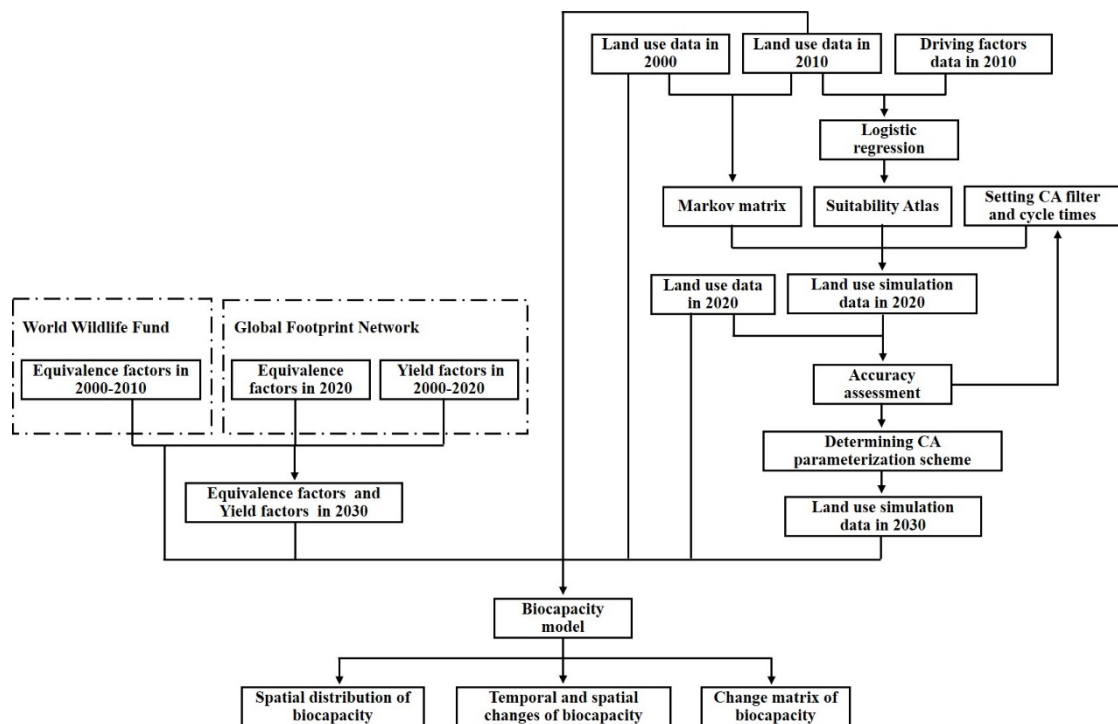


Figure 2. The main analytical framework and methods.

First, a logistic regression analysis based on the 2010 land use data and driving factor data was performed and the suitability atlas was made. Subsequently, the CA–Markov



model was used in IDRISI32 to carry out a land use scenario simulation, and the land use simulation data in 2020 was obtained. The 2020 simulation data was compared with the high-quality satellite remote sensing interpretation result (GlobeLand30 2020 data) to verify the simulation accuracy. After ensuring that the model parameterization scheme is feasible, based on the 2020 land use data, the CA–Markov model was used to carry out the 2030 land use scenario simulation. We then determined the yield factors and equivalence factors in the biocapacity model. Finally, we analyzed the spatial pattern and changing laws of biocapacity. This paper finishes with a discussion of the accuracy and uncertainty of the results and the value of government decision-making.

### 2.3.2. Logistic Regression Method

Logistic regression is a commonly used statistical method to analyze multivariate relationships [43]. As opposed to linear regression, the dependent variable of logistic regression is discrete, and there is a logical relationship between the dependent variable and the independent variable, so it is suitable for regression analysis of discrete values such as land use type [44]. Using the multiple logistic regression method, we can determine the weight of each driving factor on LUCC, exclude the factors with weak correlation, and generate suitability images of various types of land. The model is shown below [45]:

$$\text{logit}(p_i) = \ln\left(\frac{p_i}{1-p_i}\right) = a + \sum_{j=1}^n b_j x_j \quad (1)$$

where  $p_i$  is the probability of type  $i$  land appearing on the pixel;  $a$  is the regression constant;  $x_j$  is the selected  $j$ th driving factor;  $b_j$  is the regression coefficient of the variable  $x_j$ ; and the logit transformation effectively linearizes the model so that the dependent variable  $p_i$  is continuous in the range of 0–1.

### 2.3.3. CA–Markov Model

The CA model is a spatial dynamic model with discrete time, space and state, and local spatial interaction and temporal causality [46]. It is based on a regular discrete grid. Each cell has a limited number of discrete states and neighbors, and its future state depends on the state of itself and neighbors in the previous time. Using the transformation rules of cell state, we can simulate the spatial-temporal change process of land use and other complex systems [28]. The model is shown below [46]:

$$S(t+1) = F(S(t), N) \quad (2)$$

where  $S(t)$  and  $S(t+1)$  are the set of cellular states at times  $t$  and  $t+1$ , respectively;  $F$  is the transition rule of cellular state;  $N$  is the neighborhood filter.

The Markov model is a classic statistical and quantitative prediction method [47], proposed by the former Soviet Union mathematician Andrey Markov, applied in natural language processing, human resource management, land use simulation, and other fields widely. The process of using the Markov model to simulate land use change is as follows:

$$S(t+1) = P \cdot S(t) \quad (3)$$

$$P = \begin{bmatrix} p_{11} & p_{12} & \cdots & p_{1n} \\ p_{21} & p_{22} & \cdots & p_{2n} \\ \vdots & \vdots & \vdots & \vdots \\ p_{n1} & p_{n2} & \cdots & p_{nn} \end{bmatrix} \quad (4)$$

where  $S(t)$  and  $S(t+1)$  are the land use states at times  $t$  and  $t+1$ , respectively;  $P$  is the state transition probability matrix;  $p_{ij}$  is the probability of class  $i$  land transforming into class  $j$  land,  $p_{ij} \in (0, 1)$ , and  $\sum_{j=1}^n p_{ij} = 1$ , ( $i, j = 1, 2, 3, \dots, n$ ).

In the field of land use simulation, the Markov model focuses on the prediction of change quantity, but it cannot express the spatial distribution of land use or show the spatial pattern of all kinds of land change [48]; the CA model can predict the spatial-temporal change characteristics of all kinds of land [47], which makes up for the deficiency of the Markov model. The model is as follows:

$$s_{ij}(t+1) = F(s_{ij}(t), Q_{ij}(t), V) \quad (5)$$

where  $s_{ij}(t)$  and  $s_{ij}(t+1)$  are the states of the cell in row  $i$  and column  $j$  at times  $t$  and  $t+1$ , respectively;  $Q_{ij}(t)$  is the state of the neighbors of the cell in row  $i$  and column  $j$  at  $t$  time;  $V$  is the suitability atlas;  $F$  is the cell transformation rule.

#### 2.3.4. Biocapacity Model

Biocapacity is measured in global hectares (gha or  $\text{ghm}^2$ ). The biocapacity of 1 gha represents 1 ha of land with the global average productivity level. Regional biocapacity measures the biological productivity of regional land and waters [4]. The biocapacity model transforms the biocapacity into a global unified and additive biophysical index, which facilitates the study of biocapacity [16]. The model is as follows [3,5]:

$$BC = \sum_{i=1}^n A_i \times YF_i \times EQF_i \quad (6)$$

where  $BC$  is the regional biocapacity;  $n$  is the number of types of bio productive land in the region;  $A_i$  is the area of type  $i$  bio productive land (ha);  $YF_i$  is the yield factor of type  $i$  bio productive land (without unit);  $EQF_i$  is the equivalence factor of type  $i$  bio productive land (gha/ha).

In the calculation process of the biocapacity model, scientific and accurate yield factors and equivalence factors are the key parameters, which need to be determined according to the actual land use type, economic and social development stage, farming, grassland, and forestry development level of the study area, and updated in time. In the Loess Plateau in Northern Shaanxi, the unused land is generally bare desert, saline-alkali land, and sandy land. In theory, these lands still have a low level of biological production capacity, but their area is small and scattered, their output is very small, and their contribution to the total biocapacity is very small [16]. Therefore, the yield factor of unused land was set as 0 in this paper. The built-up land (such as housing area, industrial land, and infrastructure land) is mostly converted from high-quality land suitable for cultivation, but it is no longer used as bio-productive land. Therefore, this paper set its yield factor as 0. Finally, four types of land were considered in the biocapacity model: farmland, forest, grassland, and water area. The specific values of yield factors and equivalence factors can be seen in Table 2.

**Table 2.** Yield factors and equivalence factors of the Loess Plateau in Northern Shaanxi.

	2000		2010		2020		2030	
	Yield Factor	Equivalence Factor	Yield Factor	Equivalence Factor	Yield Factor	Equivalence Factor	Yield Factor	Equivalence Factor
Farmland	2.12	2.15	2.21	2.39	2.02	2.50	2.02	2.50
Forest	1.18	1.36	1.18	1.24	1.18	1.28	1.18	1.28
Grassland	0.81	0.48	0.81	0.51	0.81	0.46	0.81	0.46
Water area	1.27	0.35	1.27	0.41	1.27	0.37	1.27	0.37

In Table 2, the yield factor in 2000 and 2010 quoted the average yield factor of China in the year published by the Global Footprint Network (GFN); the yield factor in 2020 quoted the average yield factor of China in 2019 published by the GFN; the equivalence factor in 2000 quoted the average value of world equivalence factors published by the World Wildlife Fund (WWF) in 1999 and 2001; the equivalence factor in 2010 quoted the

world equivalence factor published by the WWF in 2006; the equivalence factor in 2020 quoted the world equivalence factor published by the GFN in 2019; the yield factor and equivalence factor in 2030 are assumed to be the same as in 2020.

### 3. Results and Analysis

#### 3.1. Quantity and Distribution of Land Use/Cover

Historical data and future scenario simulation results (Figure 3 and Table 3) show that the land use/cover situation in 2030 will be roughly the same as the historical period (2000, 2010, and 2020). Grassland (about 47% of the total area) and farmland (about 32% of the total area) are the main types of land of the Loess Plateau in Northern Shaanxi. The order of each type of land area is grassland > farmland > forest > unused land > built-up land > water area. The grassland is mainly distributed in the hilly and gully areas of the central and northern parts (Wuqi, Zhidan, Ansai, Zichang, Jingbian, Yuyang, Shenmu, Fugu). The farmland is mainly distributed in the riparian land in the middle and east (Jiaxian, Mizhi, Suide, Wubao, Zichang, Qingjian), the loess ridge, hill, and gully in the middle and west (Dingbian, Jingbian), and the valley terraces in the middle and south (Huangling, Fuxian, Luochuan). The forest is mainly distributed in the southern mountainous area (Baota, Ganquan, Zhidan, Yichuan). The unused land is mainly distributed in the northwest.

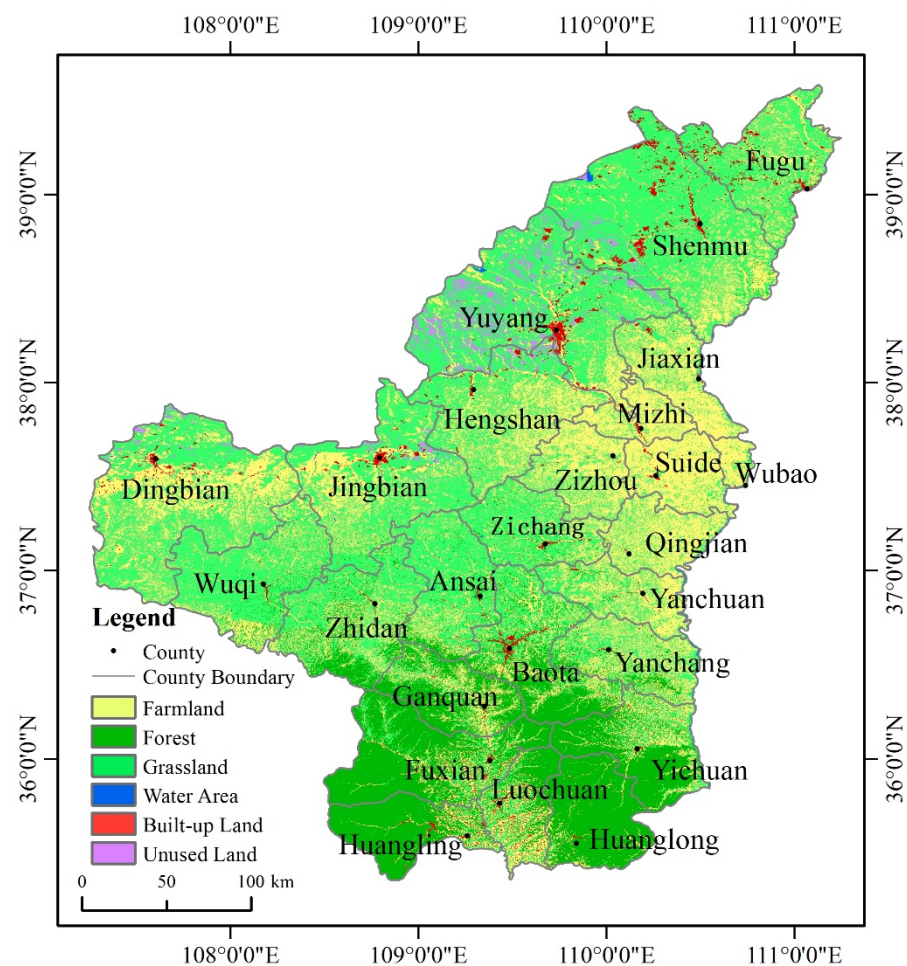


Figure 3. Land use distribution of the Loess Plateau in Northern Shaanxi in 2030.



**Table 3.** Land use area of the Loess Plateau in Northern Shaanxi in 2000–2030 (km<sup>2</sup>).

	2000	2010	2020	2030
Farmland	25,736	25,636	25,555	25,547
Forest	14,448	14,512	14,575	14,637
Grassland	37,667	37,637	37,600	37,561
Water area	311	259	228	208
Built-up land	318	479	609	716
Unused land	1581	1539	1495	1392

### 3.2. Spatial Distribution of Biocapacity

According to Formula (6), biocapacity depends on land use/cover type, the yield factor, and the equivalence factor. Therefore, the spatial distribution pattern of regional biocapacity (Figure 4) is similar to that of land use/cover under the condition of little change of yield factor and equivalence factor. The high-value area of biocapacity corresponds well with the distribution of farmland, mainly distributed in the riparian land in the middle and east, the loess ridge, hill, and gully in the middle and west, and the valley terrace in the south; the middle value corresponds well with the distribution of forest, mainly distributed in the southern mountain; the low value corresponds well with the spatial distribution of grassland, which is mainly distributed in the hilly and gully areas in the middle and north. The zero value of biocapacity is mainly distributed in the windy sandy land, saline and alkaline land in the northwest, and the central urban area of each county.

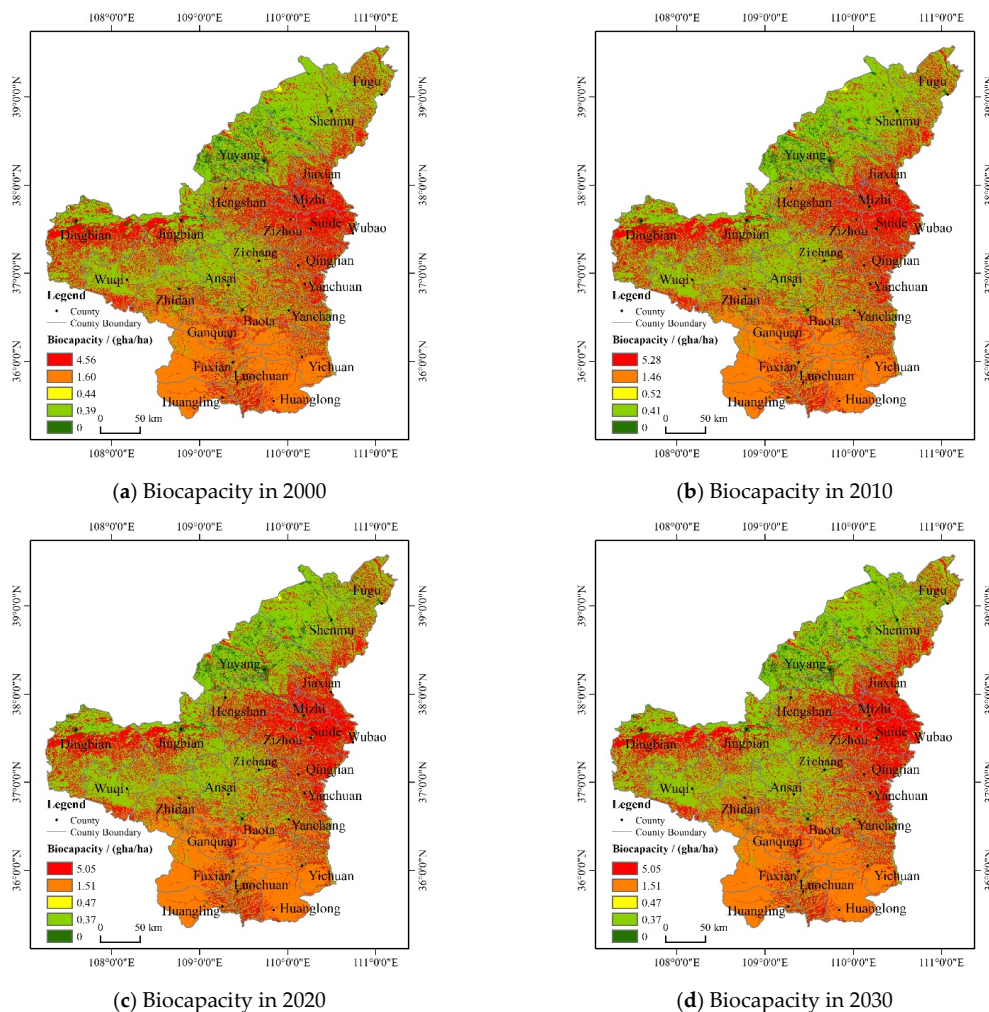


**Figure 4.** Biocapacity distribution of the Loess Plateau in Northern Shaanxi in 2000–2030.

### 3.3. Spatial-Temporal Changes of Biocapacity

By analyzing the change tendency of biocapacity in the study area (Figure 5), it can be seen that, from 2000 to 2030, the total amount of biocapacity of the Loess Plateau in Northern Shaanxi remains stable (the multi-year average value is  $1.645 \times 10^7$  gha, and the coefficient of variation is 4.26%). However, there was a significant increase of 9.98% during 2000–2010. During 2010–2020, it decreased slowly, with an amplitude of 4.14%. From 2020 to 2030, the change is small, with an increase of 0.03%. The biocapacity change of farmland and grassland is the same as the change in total biocapacity. The biocapacity change trend of the forest is as follows: decreased from 2000 to 2010 (range 8.42%), and increased from 2010 to 2020 and from 2020 to 2030 (increases of 3.67% and 0.43%, respectively). The biocapacity of the water area showed a continuous decline. Studies have shown that, continuing the changing trend in land use from 2010 to 2020, the farmland on the Loess Plateau in Northern Shaanxi will continue to decrease from 2020 to 2030, and the forest will show an increasing trend. The regional biocapacity will show a slight increase.

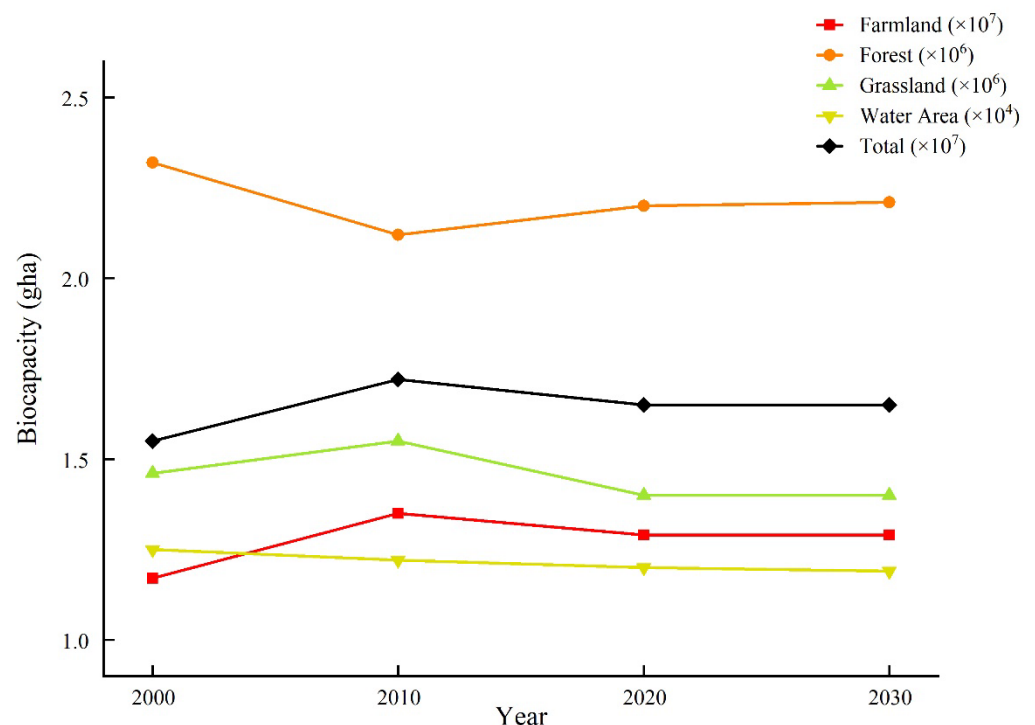


**Figure 5.** Biocapacity change tendency of the Loess Plateau in Northern Shaanxi in 2000–2030.

From the perspective of the spatial distribution pattern of biocapacity change from 2020 to 2030 (Figure 6), the areas with decreased biocapacity are mainly distributed in the middle (Ansai, Baota, Zhidan) and the north (Yuyang, Shenmu, Fugu), the main reason being that built-up land will increase, leading to the loss of farmland, grassland, and forest. In the middle (Dingbian, Wuqi) and the south (Luochuan, Huangling, Huanglong), there are more intensive descending grids. The reason for this is that the implementation of the GGP resulted in the conversion of more farmland to forest and grassland. The areas with increased biocapacity include Jiaxian, Mizhi, Zizhou, Suide, Wubao, and Qingjian in the middle and east—the reason being that these lands with low biocapacity (grassland, forest) will convert to farmland, and farmland will be more concentrated—and Zhidan in the middle, with the conversion of grassland to forest being the reason.

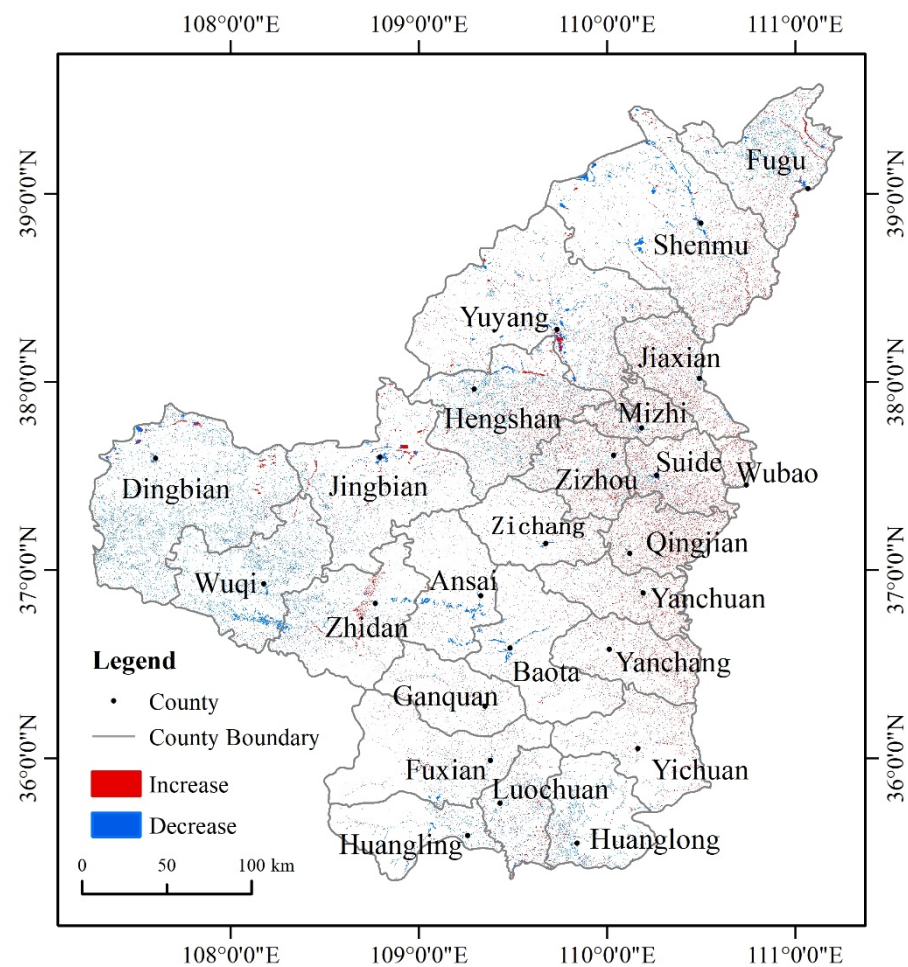


**Figure 6.** Biocapacity change of the Loess Plateau in Northern Shaanxi in 2020–2030.

### 3.4. Change Matrix of Biocapacity

Based on the analysis of the change matrix of biocapacity from 2020 to 2030 (Table 4), the overall biocapacity will increase by 4392 gha, with an increased rate of 0.03%, due to changes in land use/cover from 2020 to 2030. The land type with the largest net loss of biocapacity is farmland, with a loss of 4770 gha, accounting for 0.04% of the total biocapacity of farmland in 2020. The land type with the largest net increase in biocapacity is forest, with an increase of 9398 gha, accounting for 0.43% of the total biocapacity of forest in 2020. In addition, the increase in grassland biocapacity is greater than its transfer out, and the conversion of unused land to farmland, forest, and grassland also improves the biocapacity.

**Table 4.** Biocapacity change matrix of the Loess Plateau in Northern Shaanxi in 2020–2030.

	Biocapacity (gha)					
	Farmland	Forest	Grassland	Water Area	Built-up Land	Unused Land
Farmland	12,517,700 *	(43,417) 12,985	(330,412) 24,378	(4245) 395	(7625) 0	(1743) 0
Forest	(8849) 29,586	2,189,684 *	(2310) 570	(140) 44	(90) 0	(44) 0
Grassland	(23,830) 322,973	(1720) 6974	1,375,479 *	(312) 394	(34) 0	(612) 0
Water area	(681) 7322	(100) 321	(788) 625	8471 *	(54) 0	(568) 0
Built-up land	(0) 9722	(0) 170	(0) 216	(0) 10	0 *	(0) 0
Unused land	(0) 13068	(0) 371	(0) 1388	(0) 444	(0) 0	0 *

The value in brackets is the biocapacity of the land before the transfer in 2020, the value outside the brackets is the biocapacity of the new type of land in 2030, and “\*” indicates the conservation of biocapacity of unchanged land.

The results show that in 2020–2030, a large number of farmlands will be transferred to grassland and forest. On the one hand, this shows the continuation of the GGP in Loess Plateau and the gradual effectiveness of existing ecological projects. This change is conducive to reducing regional soil erosion, improving the local climate and ecological environment, and has important ecological significance. On the other hand, it should be noted that the rapid transfer of farmland to built-up land, and continuous and high-intensity conversion of farmland to forest and grassland, may affect regional food security.

#### 4. Discussion

##### 4.1. Simulation Accuracy Analysis

In the process of the CA–Markov simulation, the cycle number and CA filter are important parameter settings [49]. After many experiments, the authors finally decided to use a  $5 \times 5$  filter and 10 cycles, taking into account the running speed and simulation accuracy. Before the scenario simulation of land use/cover in 2030, the authors used the historical data of 2000 and 2010 to simulate the land use/cover in 2020 and compared it with the satellite remote sensing interpretation data (Globeland30 2020 data). The results show that, compared with the reference Globeland30 2020 data, the Kappa coefficient of the simulated data in 2020 is 0.9033 (it is generally believed that the simulation results are reliable when the Kappa coefficient is not less than 0.75 [50]), and there is no significant difference in the spatial distribution pattern between the simulation results and the satellite remote sensing interpretation data.

Further accuracy analysis on a pixel scale (Table 5) shows that the overall accuracy (OA) of the simulation results in 2020 is 93.77%, the user accuracy and producer accuracy of farmland, forest, and grassland are higher than 90%, the user accuracy and producer accuracy of unused land are higher than 88%, and the user accuracy of built-up land and water area is relatively low (76.67% and 79.83%, respectively). This is because the area base of built-up land and water area in the study area is very small, and a small area difference will lead to a large error ratio. Because farmland, forest, and grassland constitute the main ecosystem type of the study area (the total area of the three accounts for more than 97%), it can be considered that the CA–Markov model can meet the requirements of this research, and the selected driving factors, filter, and cycle times are reliable.

**Table 5.** Error analysis matrix for land use simulation.

	Farmland (Pixel)	Forest (Pixel)	Grassland (Pixel)	Water Area (Pixel)	Built-up Land (Pixel)	Unused Land (Pixel)	User Accuracy (%)	Producer Accuracy (%)
Farmland	2,617,1695	335,526	1,736,978	13,340	54,776	81,836	92.17	92.90
Forest	253,096	15,568,195	278,692	9031	26,460	56,827	96.15	94.17
Grassland	1,659,608	540,227	39,487,858	36,306	59,701	24,244	94.45	94.88
Water area	17,211	16,359	19,639	193,303	3168	2438	76.67	69.11
Built-up land	23,390	27,250	35,031	14,433	512,724	29,437	79.83	75.07
Unused land	46,753	44,905	59,396	13,310	26,143	1,469,643	88.52	88.30

In the simulations performed by scholars using other models, the OA of the CLUE-S model was 79.25% [51], the OA of the FLUS model reached 83% [52], and the OA of the Agent–CA model reached 90.40% [53]. In this study, the OA of the simulation result of the CA–Markov model is higher than 93.77%, which shows that the CA–Markov model has an excellent effect.

##### 4.2. Uncertainty Analysis

In terms of the selection of driving factors for LUCC, we referred to previous studies [40–42], and comprehensively considered the actual economic and social development of the study area. A total of 10 driving factors in four categories, including population density, per capita GDP, elevation, slope, precipitation, temperature, and distance to the road network, were selected. Some unconsidered secondary factors (such as agricultural



industry structure, soil types, nutrients, and real estate prices) may also affect potential changes in land use. However, if new impact factors are added in the future, they may still have an impact on the results [54].

Further analysis of the goodness of fit (Table 6) of the simplified land change driving model in this study shows that the area under the ROC curve of the logistic regression results of each category is greater than 0.87. It is believed that the explanatory power of the regression results is very good, and the selected 10 driving factors are reliable (it is generally believed that when the area under the ROC curve is not less than 0.7, the explanatory power of the regression results is good [55]).

**Table 6.** The goodness of fit analysis of regression results.

	Farmland	Forest	Grassland	Water Area	Built-Up Land	Unused Land
Per capita GDP	−0.681	0.576	−0.452	-	8.991	-
Population density	0.143	0.331	-	-	6.552	-
Elevation	−1.429	6.539	−1.190	−9.529	0.917	−1.145
Slope	0.104	-	0.222	0.380	2.698	0.301
Aspect	0.140	−0.087	-	−0.155	0.205	0.112
Annual precipitation	−1.873	7.357	−3.633	0.588	−0.208	−9.355
Annual accumulated temperature	−0.713	27.742	−9.578	−34.892	1.796	7.923
Distance to main roads	−0.449	0.208	0.242	0.477	0.106	0.596
Distance to rivers	-	−0.410	−0.301	−0.352	0.122	0.106
Distance to built-up land	-	0.193	-	−0.270	−15.090	−0.333
ROC	0.870	0.971	0.903	0.915	0.908	0.912

“-” represents that the correlation is not strong and has not been used.

The basis of the CA–Markov model simulation is to determine future land targets based on historical change laws of land use [21]. This foundation is based on the assumption that the comprehensive environmental conditions remain unchanged. If the central and local governments make major adjustments to land use policies on the Loess Plateau in Northern Shaanxi in the future, or the economic and sociological basis of land use changes undergo major changes, the simulation results of the CA–Markov model will have major deviations. Taking into account the determination of the Chinese government to carry out the construction of ecological civilization and the steady development of China’s regional economy and society, the authors believe that the GGP in the Loess Plateau will continue to be consolidated, and the level of regional economic and social development will also be steadily improved. Therefore, the environmental conditions of the Loess Plateau in Northern Shaanxi will not change significantly, and the simulation results of the CA–Markov model will be feasible. This is consistent with the research conclusions of scholars on the Loess Plateau [10,40].

In biocapacity calculations, the yield factor, the equivalence factor, and land use/cover type are the key factors. In this study, the average yield factor for China is used to represent the yield level of the Loess Plateau in Northern Shaanxi. Verification by the China Statistical Yearbook shows that China’s average production level is slightly higher than that of the Loess Plateau in Northern Shaanxi. In future research, this can be optimized in terms of regional downscaling correction of yield factors, or field measurement of yield levels. On the other hand, this study assumes that the yield factor and equivalence factor in 2030 will remain at the 2020 level. With the development of the national economy and science and technology, the overall level of biological production of various types of land will continue to increase, and the growth rate will be different. Therefore, it can be expected that the actual biocapacity in 2030 will be slightly higher than the predicted results of this study. However, on a 10-year scale, the authors believe that the changes of the above factors



will not have a significant impact on the changing trend and spatial distribution pattern of biocapacity.

#### 4.3. Policy Suggestions

From 2000 to 2020, the forest area of the Loess Plateau in Northern Shaanxi increased from  $1.45 \times 10^6$  ha to  $1.46 \times 10^6$  ha, an increase of 0.88%. In the next 10 years, it is predicted that the forest will continue to increase by 0.43%, and the biocapacity of the forest will correspondingly increase by about 9707 gha. This is the main source of the increase in the biocapacity of the Loess Plateau in Northern Shaanxi. Grassland is the ecosystem with the highest area in the Loess Plateau in Northern Shaanxi. From 2000 to 2030, the area of grassland has not changed much, but the area transferred from other land types (especially farmland and unused land) is the same as the area transferred from grassland (especially forest). This reflects the natural process of arable land being abandoned first and then naturally forming shrubs.

These changes were combined with the ecological restoration and construction project of the GGP in the Loess Plateau from 2000 to 2020 for analysis. Strongly promoted ecological protection policies are conducive to improving the coverage and biocapacity of regional forest and grassland and have a positive effect on reducing regional soil erosion, improving the local climate and the overall ecological environment [26]. It is also a prerequisite for improving the capacity of regional sustainable development and an important measure to build a “Beautiful China”. Therefore, from the perspective of environmental protection, the authors recommend that the central and local governments continue to coordinate relevant policies and continue to stably implement ecological projects such as the GGP.

However, it should be noted that ecological restoration and ecological management projects, and expansion of built-up land will lead to a decrease in farmland, especially high-quality farmland around cities. Our research shows that from 2000 to 2020, the area of farmland on the Loess Plateau in Northern Shaanxi reduced from  $2.57 \times 10^6$  ha to  $2.55 \times 10^6$  ha. In the next 10 years, it is predicted that the farmland will be reduced by about 745 ha, and the biocapacity of farmland will be reduced by 3763 gha. This is an important reason hindering the improvement of the biocapacity of the Loess Plateau in Northern Shaanxi. Therefore, to ensure regional food security and the stability of biocapacity, it is necessary to scientifically and rationally plan the conversion ratios of farmland, grassland, and forest, while increasing the degree of intensification of built-up land, and reducing the occupation of surrounding farmland by urban and rural construction.

## 5. Conclusions

In this study, we used 30-m-resolution land use/cover data from 2000, 2010, and 2020 to analyze the laws of LUCC of the Loess Plateau in Northern Shaanxi from 2000 to 2020. We comprehensively considered social development, topography, climate conditions, and spatial distance, and used the logistic regression method and CA–Markov model to simulate land use in 2030. After that, we used the biocapacity model to analyze the spatial distribution and change characteristics of regional biocapacity. Thus, we draw the following conclusions:

- (1) From 2000 to 2020, the forest of the Loess Plateau in Northern Shaanxi increased by 0.88%; the amount of grassland did not change much, but its transformation with farmland and forest reflects the process of returning farmland to grassland and developing into forest; farmland was reduced by 0.7%; forest and grassland have been well protected, and the effect of the GGP is obvious.
- (2) The biocapacity of the Loess Plateau in Northern Shaanxi increased by 9.98% from 2000 to 2010, and decreased by 4.14% from 2010 to 2020, and the total amount remained stable. It is predicted that in the next 10 years, the regional biocapacity will continue to increase by 0.03%, reaching  $16.52 \times 10^6$  gha.
- (3) To cope with the potential impact of changes in land use and biocapacity, local governments should continue to implement ecological restoration projects such as

the GGP, and rationally plan the conversion ratio of farmland, grassland, and forest to maintain regional food safety and biocapacity stability.

**Author Contributions:** Conceptualization, Y.H.; methodology, Y.H.; software, H.W.; validation, H.W.; formal analysis, H.W.; investigation, H.W.; data curation, H.W.; writing—original draft preparation, H.W.; writing—review and editing, Y.H.; visualization, H.W.; supervision, Y.H.; project administration, Y.H.; funding acquisition, Y.H. Both authors have read and agreed to the published version of the manuscript.

**Funding:** This work was funded by the National Natural Science Foundation of China (41977421), the Strategic Priority Research Program of the Chinese Academy of Sciences [XDA19040301, XDA20010202, XDA23100200], and the National Key Research and Development Plan Program of China [2016YFC0503701, 2016YFB0501502].

**Acknowledgments:** The authors would like to express their sincere thanks to the anonymous reviewers, whose comments and suggestions were of great help to improve the quality of this paper.

**Conflicts of Interest:** The authors declare no conflict of interest.

## References

- Zheng, D.; Dai, E. Environmental ethics and regional sustainable development. *J. Geogr. Sci.* **2012**, *22*, 86–92. [[CrossRef](#)]
- Kemp, R.; Parto, S.; Gibson, R.B. Governance for sustainable development: Moving from theory to practice. *Int. J. Sustain. Dev.* **2005**, *8*, 12–30. [[CrossRef](#)]
- Rees, W.E. Ecological footprints and appropriated carrying capacity: What urban economics leaves out. *Environ. Urban.* **1992**, *4*, 121–130. [[CrossRef](#)]
- Moran, D.D.; Wackernagel, M.; Kitzes, J.A.; Goldfinger, S.H.; Boutaud, A. Measuring sustainable development—Nation by nation. *Ecol. Econ.* **2008**, *64*, 470–474. [[CrossRef](#)]
- Ress, W.E.; Wackernagel, M. Ecological footprints and appropriated carrying capacity: Measuring the natural capital requirements of the human economy. *Focus* **1996**, *6*, 45–60.
- Narayana, K.A. Assessment of land parcel level planning with soil and water parameters for enhancement of Biocapacity in Gudiyattam block, Vellore District, Tamilnadu, India. *Mater. Today Proc.* **2021**, *37*, 1449–1454. [[CrossRef](#)]
- Ahmad, M.; Jiang, P.; Majeed, A.; Umar, M.; Khan, Z.; Muhammad, S. The dynamic impact of natural resources, technological innovations and economic growth on ecological footprint: An advanced panel data estimation. *Resour. Policy* **2020**, *69*, 101817. [[CrossRef](#)]
- Sarkodie, S.A. Environmental performance, biocapacity, carbon & ecological footprint of nations: Drivers, trends and mitigation options. *Sci. Total Environ.* **2021**, 751. [[CrossRef](#)]
- Usman, O.; Alola, A.A.; Sarkodie, S.A. Assessment of the role of renewable energy consumption and trade policy on environmental degradation using innovation accounting: Evidence from the US. *Renew. Energy* **2020**, *150*, 266–277. [[CrossRef](#)]
- Yue, D.; Xu, X.; Hui, C.; Xiong, Y.; Han, X.; Ma, J. Biocapacity supply and demand in Northwestern China: A spatial appraisal of sustainability. *Ecol. Econ.* **2011**, *70*, 988–994. [[CrossRef](#)]
- Gabbi, G.; Matthias, M.; Patrizi, N.; Pulselli, F.M.; Bastianoni, S. The biocapacity adjusted economic growth. Developing a new indicator. *Ecol. Indic.* **2021**, *122*, 107318. [[CrossRef](#)]
- Danish; Hassan, S.T.; Baloch, M.A.; Mahmood, N.; Zhang, J. Linking economic growth and ecological footprint through human capital and biocapacity. *Sustain. Cities Soc.* **2019**, *47*, 101516. [[CrossRef](#)]
- Niccolucci, V.; Coscieme, L.; Marchettini, N. Benefit transfer and the economic value of Biocapacity: Introducing the ecosystem service Yield factor. *Ecosyst. Serv.* **2021**, *48*, 101256. [[CrossRef](#)]
- Galli, A.; Iha, K.; Moreno Pires, S.; Mancini, M.S.; Alves, A.; Zokai, G.; Lin, D.; Murthy, A.; Wackernagel, M. Assessing the Ecological Footprint and biocapacity of Portuguese cities: Critical results for environmental awareness and local management. *Cities* **2020**, *96*, 102442. [[CrossRef](#)]
- Zhang, S.; Shi, Q.; Cheng, M. Renewable natural capital, the Biocapacity, and subjective well-being. *J. Clean. Prod.* **2017**, *150*, 277–286. [[CrossRef](#)]
- Monfreda, C.; Wackernagel, M.; Deumling, D. Establishing national natural capital accounts based on detailed Ecological Footprint and biological capacity assessments. *Land Use Policy* **2004**, *21*, 231–246. [[CrossRef](#)]
- Rees, W.E. Revisiting carrying capacity: Area-based indicators of sustainability. *Popul. Environ.* **1996**, *17*, 195–215. [[CrossRef](#)]
- Verburg, P.H.; Soepboer, W.; Veldkamp, A.; Limpiada, R.; Espaldon, V.; Mastura, S.S.A. Modeling the spatial dynamics of regional land use: The CLUE-S model. *Environ. Manag.* **2002**, *30*, 391–405. [[CrossRef](#)] [[PubMed](#)]
- Liu, X.; Li, X.; Ai, B.; Tao, H.; Wu, S.; Liu, T. Multi-agent systems for simulating and planning land use development. *Acta Geogr. Sin.* **2006**, *61*, 1101–1112.
- Liu, X.; Liang, X.; Li, X.; Xu, X.; Ou, J.; Chen, Y.; Li, S.; Wang, S.; Pei, F. A future land use simulation model (FLUS) for simulating multiple land use scenarios by coupling human and natural effects. *Landsc. Urban Plan.* **2017**, *168*, 94–116. [[CrossRef](#)]

21. Yagoub, M.M.; Al Bizreh, A.A. Prediction of Land Cover Change Using Markov and Cellular Automata Models: Case of Al-Ain, UAE, 1992–2030. *J. Indian Soc. Remote Sens.* **2014**, *42*, 665–671. [[CrossRef](#)]
22. Wu, J.; Feng, Z.; Gao, Y.; Huang, X.; Liu, H.; Huang, L. Recent progresses on the application and improvement of the CLUE-S model. *Prog. Geogr.* **2012**, *31*, 3–10.
23. Li, S.; Liu, X.; Li, X.; Chen, Y. Simulation model of land use dynamics and application: Progress and prospects. *J. Remote Sens.* **2017**, *21*, 329–340.
24. Yang, Q.; Li, X.; Liu, X. Urban land use change research based on Agent and Cellular Automata. *J. Geo Inf. Sci.* **2005**, *7*, 78–81.
25. Gao, M.; Xiao, Y.; HU, Y. Evaluation of Water Yield and Soil Erosion in the Three-River-Source Region under Different Land-Climate Scenarios. *J. Resour. Ecol.* **2020**, *11*, 13–26.
26. Hu, Y.; Gao, M. Batunacun, Evaluations of water yield and soil erosion in the Shaanxi-Gansu Loess Plateau under different land use and climate change scenarios. *Environ. Dev.* **2020**, *34*, 100488. [[CrossRef](#)]
27. Guan, D.; Gao, W.; Watari, K.; Fukahori, H. Land use change of Kitakyushu based on landscape ecology and Markov model. *J. Geogr. Sci.* **2008**, *18*, 455–468. [[CrossRef](#)]
28. Li, X.; Yeh, A.G.-O. Neural-network-based cellular automata for simulating multiple land use changes using GIS. *Int. J. Geogr. Inf. Sci.* **2002**, *16*, 323–343. [[CrossRef](#)]
29. Zhang, F.; Kung, H.T.; Johnson, V.C. Assessment of Land-Cover/Land-Use Change and Landscape Patterns in the Two National Nature Reserves of Ebinur Lake Watershed, Xinjiang, China. *Sustainability* **2017**, *9*, 724. [[CrossRef](#)]
30. Sang, L.; Zhang, C.; Yang, J.; Zhu, D.; Yun, W. Simulation of land use spatial pattern of towns and villages based on CA–Markov model. *Math. Comput. Model.* **2011**, *54*, 938–943. [[CrossRef](#)]
31. Fu, B.; Chen, L.; Ma, K.; Zhou, H.; Wang, J. The relationships between land use and soil conditions in the hilly area of the loess plateau in northern Shaanxi, China. *CATENA* **2000**, *39*, 69–78. [[CrossRef](#)]
32. Hu, Y.; Dao, R.; Hu, Y. Vegetation change and driving factors: Contribution analysis in the loess plateau of China during 2000–2015. *Sustainability* **2019**, *11*, 1320. [[CrossRef](#)]
33. Fu, B.; Liu, Y.; Lü, Y.; He, C.; Zeng, Y.; Wu, B. Assessing the soil erosion control service of ecosystems change in the Loess Plateau of China. *Ecol. Complex.* **2011**, *8*, 284–293. [[CrossRef](#)]
34. Lu, Y.H.; Fu, B.J.; Feng, X.M.; Zeng, Y.; Liu, Y.; Chang, R.Y.; Sun, G.; Wu, B.F. A Policy-Driven Large Scale Ecological Restoration: Quantifying Ecosystem Services Changes in the Loess Plateau of China. *PLoS ONE* **2012**, *7*, e31782.
35. Chen, J.; Ban, Y.; Li, S. Open access to Earth land-cover map. *Nature* **2014**, *514*, 434.
36. Tsendbazar, N.E.; Herold, M.; de Bruin, S.; Lesiv, M.; Fritz, S.; Van De Kerchove, R.; Buchhorn, M.; Duerauer, M.; Szantoi, Z.; Pekel, J.F. Developing and applying a multi-purpose land cover validation dataset for Africa. *Remote Sens. Environ.* **2018**, *219*, 298–309. [[CrossRef](#)]
37. Shafizadeh-Moghadam, H.; Minaei, M.; Feng, Y.; Pontius, R.G. GlobeLand30 maps show four times larger gross than net land change from 2000 to 2010 in Asia. *Int. J. Appl. Earth Obs. Geoinf.* **2019**, *78*, 240–248. [[CrossRef](#)]
38. Rudke, A.P.; Fujita, T.; de Almeida, D.S.; Eiras, M.M.; Xavier, A.C.F.; Rafee, S.A.A.; Santos, E.B.; de Moraes, M.V.B.; Martins, L.D.; de Souza, R.V.A.; et al. Land cover data of Upper Parana River Basin, South America, at high spatial resolution. *Int. J. Appl. Earth Obs. Geoinf.* **2019**, *83*, 101926. [[CrossRef](#)]
39. Feng, Y.; Lei, Z.; Tong, X.; Gao, C.; Chen, S.; Wang, J.; Wang, S. Spatially-explicit modeling and intensity analysis of China’s land use change 2000–2050. *J. Environ. Manag.* **2020**, *263*, 110407. [[CrossRef](#)] [[PubMed](#)]
40. Li, K.; Feng, M.; Biswas, A.; Su, H.; Niu, Y.; Cao, J. Driving Factors and Future Prediction of Land Use and Cover Change Based on Satellite Remote Sensing Data by the LCM Model: A Case Study from Gansu Province, China. *Sensors* **2020**, *20*, 2757. [[CrossRef](#)]
41. Ullah, S.; Ahmad, K.; Sajjad, R.U.; Abbasi, A.M.; Nazeer, A.; Tahir, A.A. Analysis and simulation of land cover changes and their impacts on land surface temperature in a lower Himalayan region. *J. Environ. Manag.* **2019**, *245*, 348–357. [[CrossRef](#)]
42. Zhang, Y.; Hu, Y.; Zhuang, D. A highly integrated, expandable, and comprehensive analytical framework for urban ecological land: A case study in Guangzhou, China. *J. Clean. Prod.* **2020**, *268*, 122360. [[CrossRef](#)]
43. He, D.; Jin, F.; Zhou, J. The changes of land use and landscape pattern based on Logistic-CA-Markov model: A case study of Beijing-Tianjin-Hebei metropolitan region. *Sci. Geogr. Sin.* **2011**, *31*, 903–910.
44. Sarkar, T.; Mishra, M. Soil Erosion Susceptibility Mapping with the Application of Logistic Regression and Artificial Neural Network. *J. Geovis. Spat. Anal.* **2018**, *2*, 8. [[CrossRef](#)]
45. Shahbazian, Z.; Faramarzi, M.; Rostami, N.; Mahdizadeh, H. Integrating logistic regression and cellular automata-Markov models with the experts’ perceptions for detecting and simulating land use changes and their driving forces. *Environ. Monit. Assess.* **2019**, *191*, 17. [[CrossRef](#)] [[PubMed](#)]
46. Wolfram, S. Statistical mechanics of cellular automata. *Rev. Mod. Phys.* **1983**, *55*, 601. [[CrossRef](#)]
47. Wijesekera, G.N.; Gupta, A.; Valeo, C.; Hasbani, J.G.; Qiao, Y.; Delaney, P.; Marceau, D.J. Assessing the impact of future land-use changes on hydrological processes in the Elbow River watershed in southern Alberta, Canada. *J. Hydrol.* **2012**, *412–413*, 220–232. [[CrossRef](#)]
48. Nor, A.N.M.; Corstanje, R.; Harris, J.A.; Brewer, T. Impact of rapid urban expansion on green space structure. *Ecol. Indic.* **2017**, *81*, 274–284. [[CrossRef](#)]
49. Pan, Y.; Roth, A.; Yu, Z.; Doluschitz, R. The impact of variation in scale on the behavior of a cellular automata used for land use change modeling. *Comput. Environ. Urban Syst.* **2010**, *34*, 400–408. [[CrossRef](#)]

50. Visser, H.; de Nijs, T. The Map Comparison Kit. *Environ. Model. Softw.* **2006**, *21*, 346–358. [[CrossRef](#)]
51. Peng, K.; Jiang, W.; Deng, Y.; Liu, Y.; Wu, Z.; Chen, Z. Simulating wetland changes under different scenarios based on integrating the random forest and CLUE-S models: A case study of Wuhan Urban Agglomeration. *Ecol. Indic.* **2020**, *117*, 106671. [[CrossRef](#)]
52. Guo, H.; Cai, Y.; Yang, Z.; Zhu, Z.; Ouyang, Y. Dynamic simulation of coastal wetlands for Guangdong-Hong Kong-Macao Greater Bay area based on multi-temporal Landsat images and FLUS model. *Ecol. Indic.* **2021**, *125*, 107559. [[CrossRef](#)]
53. Liu, D.; Zheng, X.; Wang, H. Land-use Simulation and Decision-Support system (LandSDS): Seamlessly integrating system dynamics, agent-based model, and cellular automata. *Ecol. Model.* **2020**, *417*, 108924. [[CrossRef](#)]
54. He, C.; Okada, N.; Zhang, Q.; Shi, P.; Li, J. Modelling dynamic urban expansion processes incorporating a potential model with cellular automata. *Landsc. Urban Plan.* **2008**, *86*, 79–91. [[CrossRef](#)]
55. Pontius, R.G.; Schneider, L.C. Land-cover change model validation by an ROC method for the Ipswich watershed, Massachusetts, USA. *Agric. Ecosyst. Environ.* **2001**, *85*, 239–248. [[CrossRef](#)]